Wafer-Scale Integration of Graphene-based Electronic, Optoelectronic and Electroacoustic Devices —Supplementary Information

He Tian,[1,2] Yi Yang,[1,2] Dan Xie,[1,2] Ya-Long Cui,[1,2] Wen-Tian Mi,[1,2]

Yuegang Zhang,[3,4,] Tian-Ling Ren[1,2,*]*

[1]Institute of Microelectronics, Tsinghua University, Beijing 100084, China

[2]Tsinghua National Laboratory for Information Science and Technology (TNList), Tsinghua University, Beijing 100084, China

[3]The Molecular Foundry, Lawrence Berkeley National Laboratory, 1 Cyclotron Road, Berkeley, CA 94720, USA

[4]Suzhou Institute of Nano-Tech and Nano-Bionics, Chinese Academy of Sciences, Suzhou 215123, China

*Corresponding Author E-mail: RenTL@tsinghua.edu.cn, yzhang5@lbl.gov

This file includes:

1. XPS, optical and electrical results of laser scribed graphene
2. Capacitance and mobility of the laser scribed graphene in-plane transistors
3. Turn on/off time and working principle of the laser scribed graphene photodetectors
4. Measure distance relation and working principle of the laser scribed graphene loudspeakers

1. XPS, optical and electrical results of laser scribed graphene

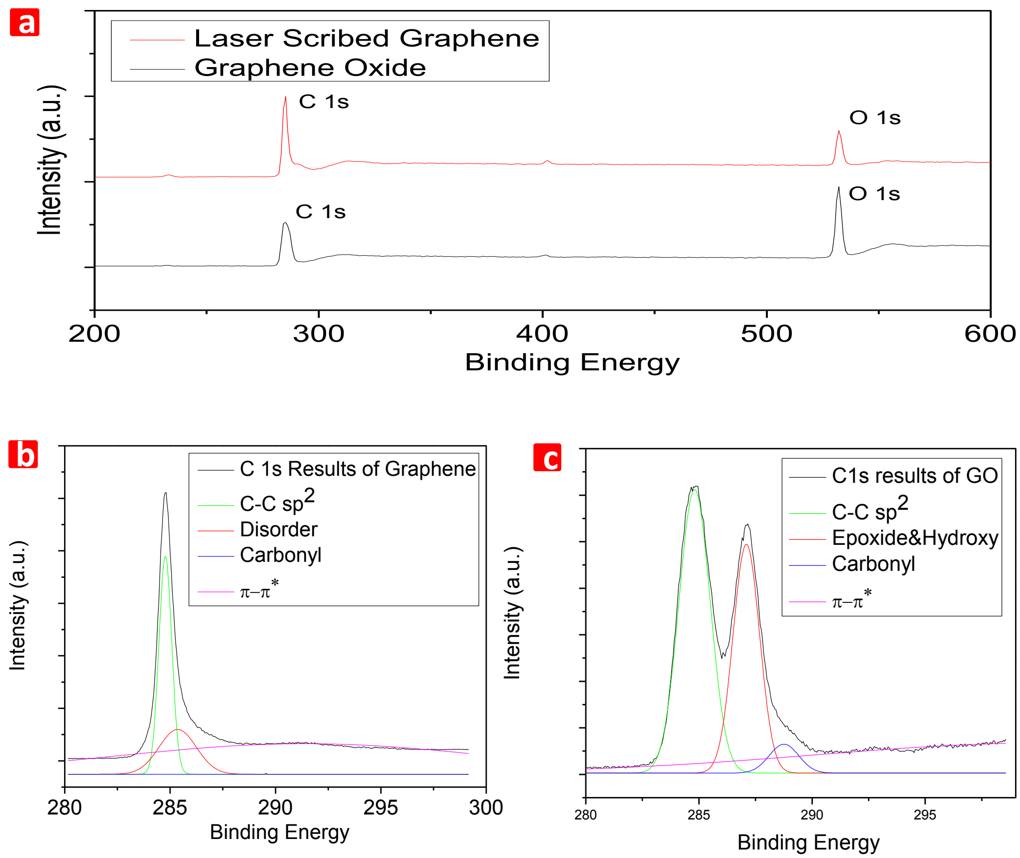

Figure S1. XPS Results of laser scribed graphene and graphene oxide. (a) The full spectrum of the laser scribed graphene and graphene oxide. Compared with graphene oxide, it is noticed that oxygen is reduced significantly in laser scribed graphene. (b) C1s spectrum and fitting peaks of the laser scribed graphene. (c) C1s spectrum and fitting peaks of the GO film. Compared with graphene oxide, it is also noticed that the C-C sp^2 and π-π* bonding enhance significantly after reduction.

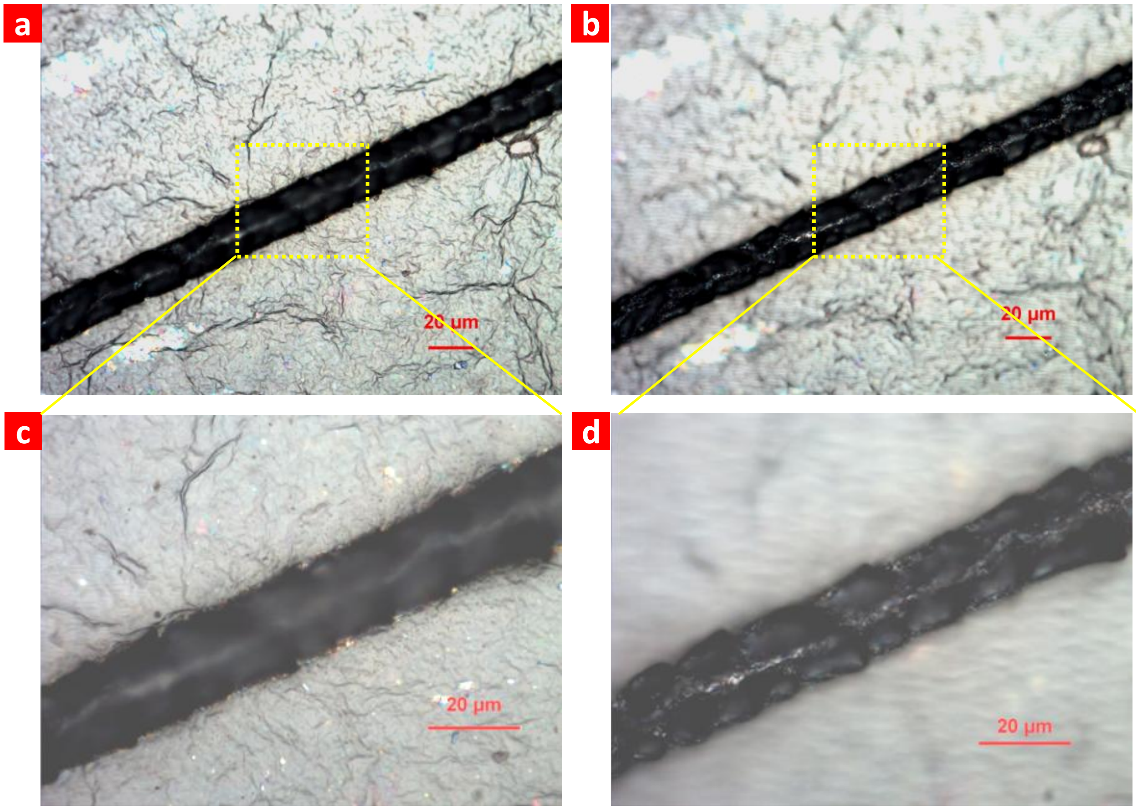

Figure S2. The laser scribed graphene micro-ribbon with a minimum patterning resolution of 20 μm. (a) An optical image of laser scribed graphene micro-ribbon under low magnification focused on the GO film. (b) An optical image of laser scribed graphene micro-ribbon under low magnification focused on the laser scribed graphene. (c) A zoom in optical image of laser scribed graphene micro-ribbon under high magnification focused on the GO film. (d) A zoomed-in optical image of laser scribed graphene micro-ribbon under high magnification focused on the laser scribed graphene.

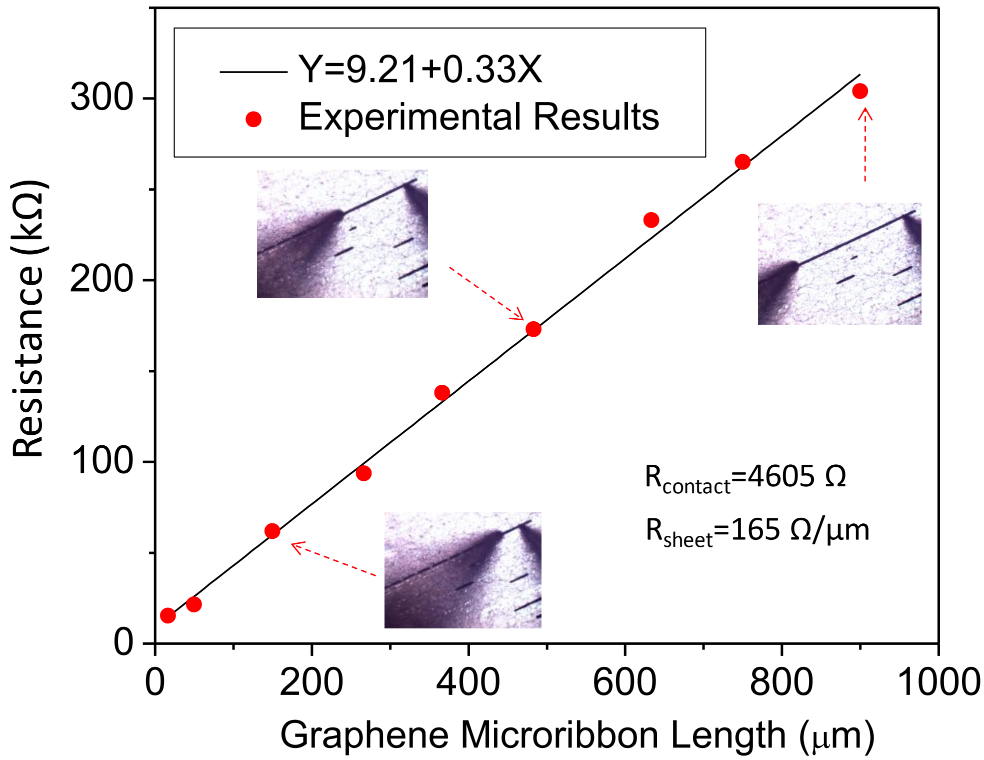

Figure S3. Two-probe measurement of the laser scribed graphene micro-ribbon with 20 µm width. Through the fitting line, the contact resistance is estimated 4605 Ω and the sheet resistance of the graphene is about 165 Ω/squre.

2. Capacitance and mobility of the laser scribed graphene in-plane transistors

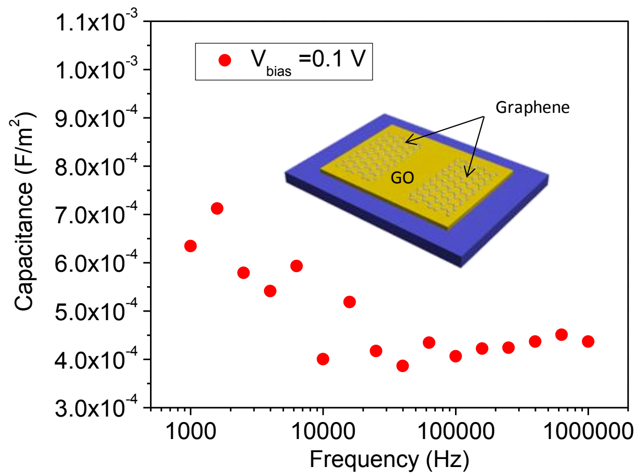

Figure S4. Frequency dependence of the specific capacitance of the capacitor in graphene/GO/graphene in-plane configuration.

The room-temperature mobility for electrical transport (Fig.4b) is calculated based on the following equations (Eq. S1). The physical parameters and values are listed in Table S1.

$$\mu = \frac{\Delta I_{SD}}{\Delta V_{SG}} \cdot \frac{L}{W} \cdot \frac{1}{V_{SD} \cdot C_S} \tag{S1}$$

Table S1: Calculation Parameters for graphene in-plane transistors

Symbol	Physical significance	Values
L	Graphene channel length	200 μm
W	Graphene channel width	100 μm
t	GO dielectric thickness	150 μm
V_{SD}	Source-drain bias voltage	0.1 V
I_{SD}	Source-drain current	3 μA to 0.5 μA
V_{SG}	Source-gate bias voltage	-40 V to +40 V
$\Delta I_{SD}/\Delta V_{SG}$	The slope of the I-V characteristic as shown in Fig. 5(a)	Holes: 3.13×10^{-8}
C_S	Capacitance per area of the SiO_2 dielectric.	6.34×10^{-4} $F\cdot m^{-2}$
e	Elementary charge	1.602×10^{-19} C
μ	Field effect carrier mobility	Holes: 9.87 $cm^2\cdot V^{-1}\cdot s^{-1}$

3. Turn on/off time and working principle of the laser scribed graphene photodetectors

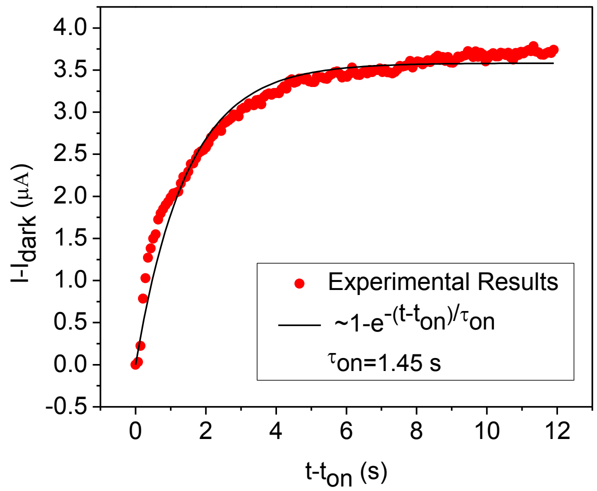

Figure S5. The current response to turning on of incident light in showing exponential rise behaviors with second time scales.

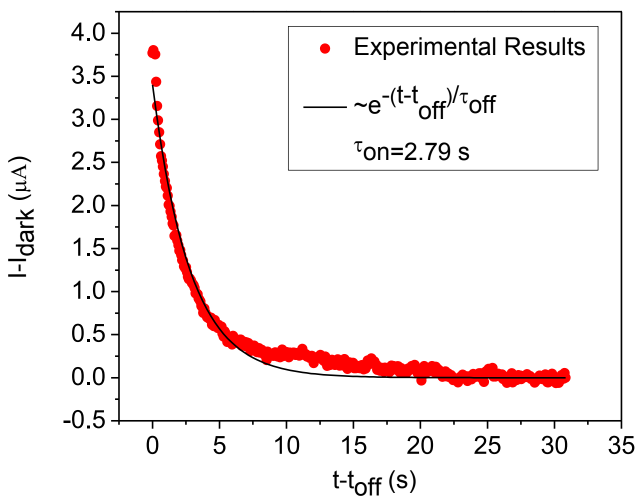

Figure S6. The current response to turning OFF of incident light in showing exponential fall behaviors with second time scales.

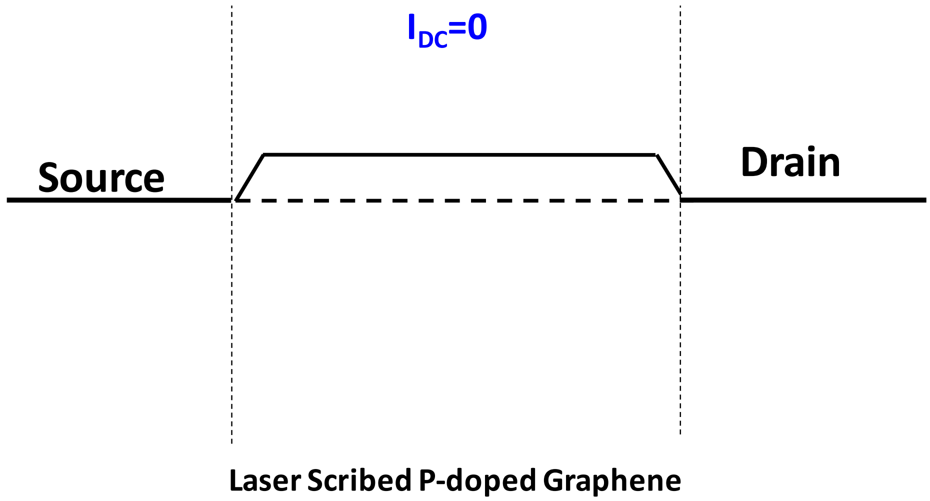

Figure S7. Energy band diagram of a laser scribed graphene.

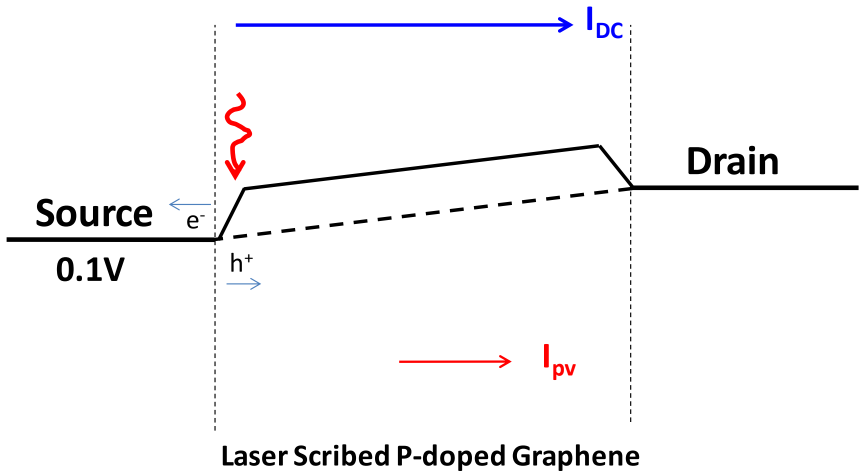

Figure S8. Energy band diagram of a laser scribed graphene with 0.1 V bias after laser illumination.

One of the important factors to evaluate the performance of the photodetectors is the photo responsivity. The responsivity (R_{λ}) is written as

$$R_{\lambda} = \frac{\Delta I}{S \times P_{in}} \tag{S2}$$

Where ΔI , S , P_{in} are photocurrent, device area, and optical power per unit area, respectively.

Another figure of the merit of photodetectors is the specific detectivity (D^*), which measures the sensitivity of the device written as

$$D^* = \frac{(S)^{1/2} R_{\lambda}}{(2eI_{dark})^{1/2}} \tag{S3}$$

Where S , R_{λ} , e , I_{dark} are device area, responsivity, electron charge and dark current, respectively.

The physical parameters and values are listed in Table S2.

Table S2: Calculation Parameters for graphene photodetectors

Symbol	Physical significance	Values
L	Graphene channel length	5 mm
W	Graphene channel width	10 mm
V_{bias}	Bias voltage	0.1 V
I_{dark}	Current in dark	64.02 µA
I_{light}	Current in light	67.59 µA
ΔI	Photo current	3.57 µA
P	Laser power intensity	221 mW/m^2
e	Elementary charge	1.602×10^{-19} C
R_λ	Photo responsivity	0.32 A/W
D^*	Photo specific detectivity	4.996×10^{10} $cmHz^{1/2}W^{-1}$

4. Measure distance relation and working principle of the laser scribed graphene loudspeakers

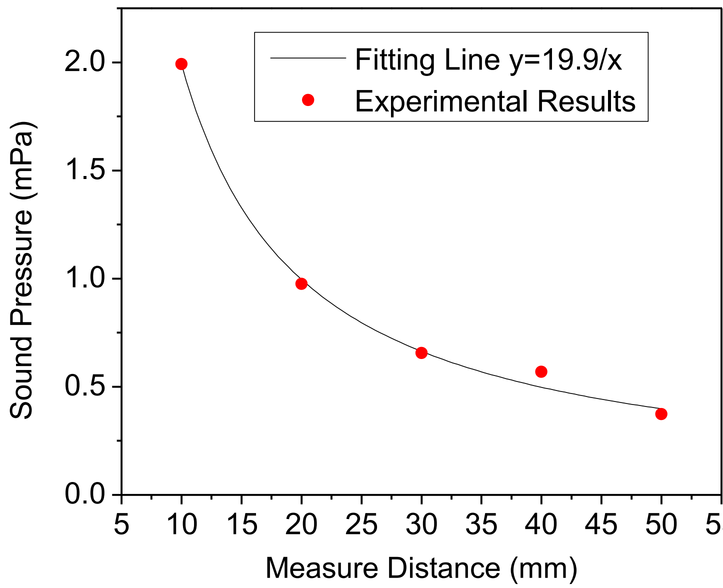

Figure S9. The plot of the sound pressure versus the measure distance (distance from loudspeaker to microphone) at 20 kHz sound frequency. The line indicates that there is an inverse relationship between the output sound pressure and measure distance.

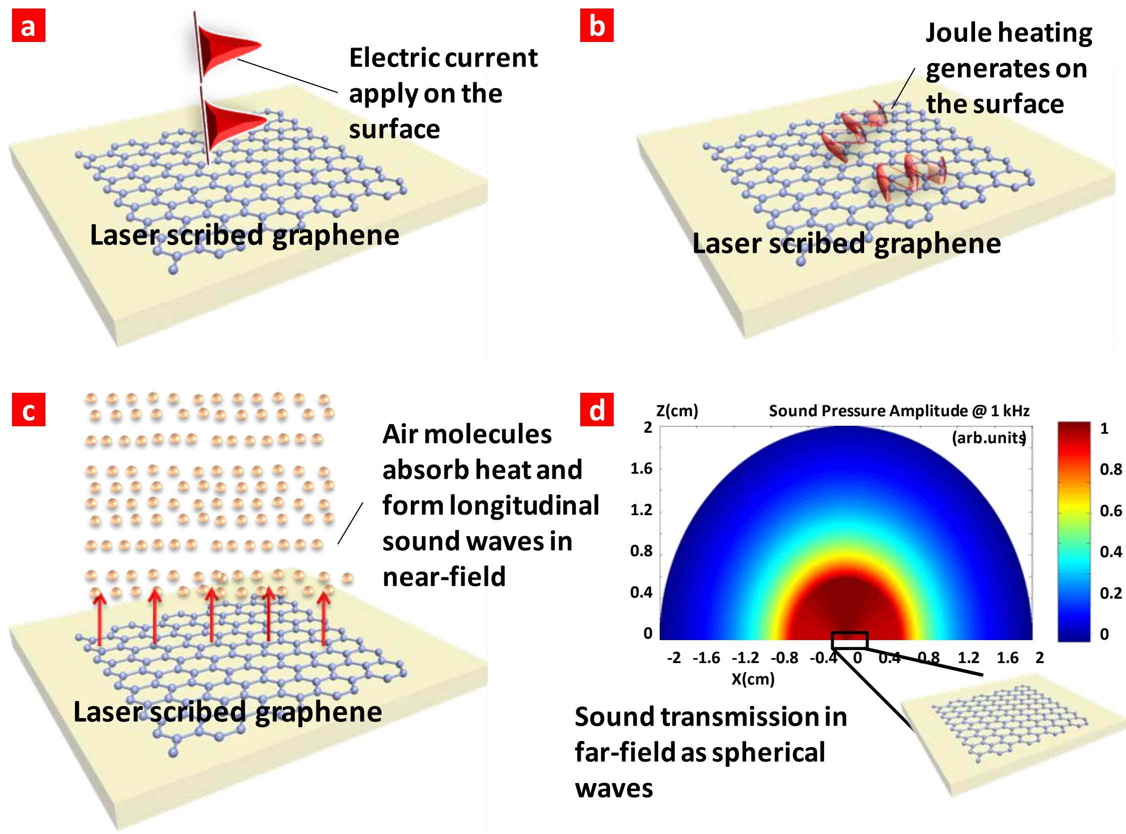

Figure S10. Schematic diagram of the mechanism for sound generation from laser scribed graphene. (a) Applying electric current through the surface of laser scribed graphene. (b) Generation of Joule heating on the surface of laser scribed graphene. (c) Longitudinal sound waves formation in the near-field. (d) Spherical sound waves transmission in the far-field.